environmental microbiology

Environmental Microbiology (2015) **17**(4), 1321–1337 doi:10.1111/1462-2920.12581

The meningococcal autotransporter AutA is implicated in autoaggregation and biofilm formation

Jesús Arenas,[1]* Sara Cano,[1] Reindert Nijland,[2] Vérène van Dongen,[1] Lucy Rutten,[3] Arie van der Ende[4,5] and Jan Tommassen[1]

[1]*Department of Molecular Microbiology and Institute of Biomembranes and* [3]*Section Cellular Architecture and Dynamics, Department of Biology, Utrecht University, Paudalaan 8, Utrecht 3584 CH, The Netherlands.*

[2]*Department of Medical Microbiology, University Medical Center Utrecht, Utrecht, The Netherlands.*

[4]*Department of Medical Microbiology, Academic Medical Center, Amsterdam, The Netherlands.*

[5]*Netherlands Reference Laboratory for Bacterial Meningitis, Academic Medical Center, Amsterdam, The Netherlands.*

Summary

Autotransporters (ATs) are proteins secreted by Gram-negative bacteria that often play a role in virulence. Eight different ATs have been identified in *Neisseria meningitidis*, but only six of them have been characterized. AutA is one of the remaining ATs. Its expression remains controversial. Here, we show that the *autA* gene is present in many neisserial species, but its expression is often disrupted by various genetic features; however, it is expressed in certain strains of *N. meningitidis*. By sequencing the *autA* gene in large panels of disease isolates and Western blot analysis, we demonstrated that AutA expression is prone to phase variation at AAGC nucleotide repeats located within the DNA encoding the signal sequence. AutA is not secreted into the extracellular medium, but remains associated with the bacterial cell surface. We further demonstrate that AutA expression induces autoaggregation in a process that, dependent on the particular strain, may require extracellular DNA (eDNA). This property influences the organization of bacterial communities like lattices and biofilms. *In vitro* assays evidenced that AutA is a self-associating AT that binds DNA. We suggest that AutA-mediated autoaggregation might be particularly important for colonization and persistence of the pathogen in the nasopharynx of the host.

Received 30 November, 2013; accepted 22 July, 2014. *For correspondence. E-mail J.A.ArenasBusto@uu.nl; Tel. (+31) 30 2533017; Fax (+31) 30 2532837.

Introduction

The Gram-negative bacterium *Neisseria meningitidis* normally resides as a commensal in the nasopharynx without causing any symptoms. However, occasionally, it may reach the blood stream and cerebrospinal fluid by crossing epithelial and endothelial barriers, and cause sepsis and/or meningitis. Vaccines based on capsular polysaccharides are effective in conferring immunity but not against strains of serogroup B because of low immunogenicity of the corresponding polysaccharide. Vaccines based on non-capsular antigens were developed, but a definite formulation is still not available mainly because of diverse immune-evasion strategies of the bacterium, including phase variation, which is a reversible turning on and off of protein expression (Saunders *et al*., 2000; Tauseef *et al*., 2013), antigenic variation (Virji, 2009) and/or variable accessibility of non-capsular surface structures (Arenas *et al*., 2008). Thus, meningococcal infection remains a worldwide problem and requires better understanding of the role of surface-exposed structures.

In the nasopharynx, meningococci form microcolonies (Sim *et al*., 2000). These structures, which resemble biofilms (Costerton *et al*., 1995), confer protection against hostile environmental conditions. The generation, development and dispersal of biofilms are governed by various surface-exposed structures, whose expression is often regulated by different mechanisms. Type IV pili, the heparin-binding lipoprotein NHBA and the α-peptide of the autotransporter (AT) immunoglobulin A (IgA) protease have been implicated in biofilm formation. Expression of type IV pili is phase variable (Criss *et al*., 2005) while the surface exposure of NHBA and the α-peptide of IgA protease is regulated via proteolytic cleavage by the phase-variable AT NalP (Serruto *et al*., 2010; Arenas *et al*., 2013; Roussel-Jazédé *et al*., 2014). The initiation of biofilm formation requires extracellular DNA (eDNA) in most meningococcal strains, but strains of clonal complexes (cc) 8 and 11 have evolved an eDNA-independent strategy (Lappann *et al*., 2010; Arenas *et al*., 2013). Capsular polysaccharides have

been shown to inhibit biofilm formation on abiotic surfaces (Yi *et al*., 2004; Lappann and Vogel, 2010); their expression can be downregulated after attachment. Thus, the regulated expression of surface-exposed structures confers the possibility to vary between microcolony formation and planktonic cells, favouring colonization of new hosts or ecological niches.

We are studying the possible involvement of ATs in biofilm formation. ATs consist of an N-terminal signal sequence, a secreted passenger domain and a translocator domain (Grijpstra *et al*., 2013). The signal sequence directs transport of the protein across the inner membrane, while the translocator domain integrates into the outer membrane and mediates the translocation of the passenger to the cell surface. The translocator domain of classical monomeric ATs forms a 12-stranded β-barrel. In trimeric ATs, it is shorter and each subunit contributes four β-strands to form together a similar 12-stranded β-barrel (Grijpstra *et al*., 2013). A small C-terminal segment of the passenger of classical ATs, called autochaperone domain, is first translocated and supposedly folds at the extracellular side, thereby helping the translocation and folding of the rest of passenger (Oliver *et al*., 2003; Peterson *et al*., 2010). Once located at the cell surface, the passenger can be proteolytically released by an autocatalytic event or by other proteases, or it remains attached to the cells. The passenger domains of different ATs are highly variable and can exert a large variety of functions (Grijpstra *et al*., 2013).

Previously, eight genes encoding ATs were identified, at that time, in the available meningococcal genome sequences (van Ulsen and Tommassen, 2006). In strain MC58, six ATs are expressed, i.e. AusI, App, IgA protease, NalP, NhhA and NadA. These ATs have been characterized to a considerable extent (Serruto *et al*., 2003; van Ulsen *et al*., 2003; 2006; Capecchi *et al*., 2005; Vidarsson *et al*., 2005; Scarselli *et al*., 2006; van Ulsen and Tommassen, 2006). The former four are classical monomeric ATs with protease activities and are released into the extracellular milieu, while NhhA and NadA are trimeric ATs that remain attached to the cell surface after secretion. Most of them are implicated in virulence, e.g. by mediating interactions with eukaryotic cells (Lin *et al*., 1997; Serruto *et al*., 2003; Capecchi *et al*., 2005; Vidarsson *et al*., 2005; Scarselli *et al*., 2006). The expression of two of these ATs, NalP and AusI, is phase variable by a slipped-strand mispairing mechanism (Turner *et al*., 2002; van Ulsen and Tommassen, 2006).

The remaining two ATs, i.e. AutA and AutB, have been poorly characterized so far. They were first described by Peak and colleagues (1999) and Ait-Tahar and colleagues (2000). AutA was reported to be a potent $CD4^+$ T-cell and B-cell stimulating antigen (Ait-Tahar *et al*., 2000). Its expression was suggested to be prone to phase variation due to the presence of a tetranucleotide repeat (AAGC) located immediately downstream of the start codon in the signal-sequence-encoding part of the gene (Peak *et al*., 1999). Based on Western blotting assays, expression of AutA was suggested in several *N. meningitidis* strains including MC58 and Z2491 (Ait-Tahar *et al*., 2000). However, *autA* is a pseudogene in these strains because of the presence of a premature stop codon in the correct reading frame preventing expression even if the gene is in the on phase at the tetranucleotide repeat (Peak *et al*., 1999; van Ulsen and Tommassen, 2006). In the present study, we characterized its expression in a large panel of *N. meningitidis* strains and describe its possible function.

Results

Characterization and distribution of the autA gene

Previously, the *autA* gene was identified in the neisserial genome sequences available at that time, i.e. from three strains of *N. meningitidis*, one of *N. lactamica* and one of *N. gonorrhoeae* (van Ulsen and Tommassen, 2006). In all these genome sequences, *autA* was found to be disrupted by phase variation and, in the meningococcal sequences, also by the presence of a premature stop codon in the correct reading frame. The gonococcal *autA* additionally contained a large deletion of ~1000 bp. Because genome sequences from a large number of *Neisseria* spp. are currently available, we decided to extend this analysis to gain more insight in the possible expression of *autA*. Using Blast searches and genome comparisons, the gene was identified in the now available genome sequences of *N. meningitidis*, *N. gonorrhoeae*, *N. lactamica*, *N. flavescens* and *N. polysaccharea* strains. Figure S1A illustrates the representative genomic context in some of the genomes, and Table S1 lists the genetic characteristics of *autA* in a panel of 81 *neisserial* genome sequences.

The genomic context of the *autA* genes is nearly identical in all available genome sequences except in *N. flavescens*, where the gene is placed in a completely different position (Fig. S1A). The *autA* gene sequences revealed a variable number of AAGC nucleotide repeats immediately downstream of the start codon that renders the gene in frame in 28% of the meningococcal ($n = 58$), 18% of the gonococcal ($n = 17$), 50% of the *N. lactamica* ($n = 4$), 100% of the *N. flavescens* ($n = 1$) and 100% of the *N. polysaccharea* ($n = 1$) strains. Interestingly, the repeat unit in *N. lactamica* strain NS19 was AGGC. *Neisseria meningitidis* presented the highest variability with respect to the number of repeat units ranging from 6 to 40 (Table S1). Even if the gene remained in frame at the AAGC repeats, it could not always be expressed because it was disrupted further downstream in many strains by

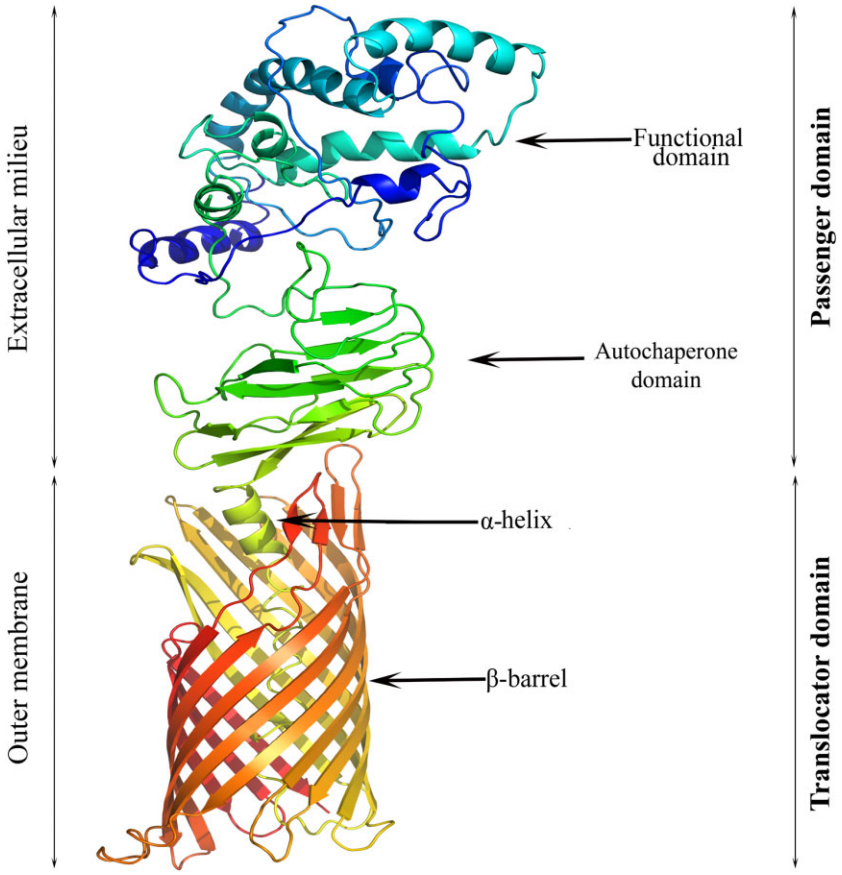

Fig. 1. Predicted structural model for AutA of MC58. The structures of the translocator domain, passenger and autochaperone domain were predicted independently.

premature stop codon(s), short deletions or insertions that changed the reading frame, or more extensive insertions or deletions. Such disruptions were found in 76% of the meningococcal strains, all gonococcal strains and *N. flavescens* NRL30031/H210 (Table S1). To summarize, of 58 meningococcal genomes examined here, only five (8.6%) are expected to express AutA, i.e. α14 and M01-240355 of cc 53 and 213, respectively, and 93004, α704 and NM2795 of unknown cc. Another nine strains, including one of cc4821 and two of the three cc269 strains examined, may express a full-length AutA if phase variation occurs at the tetranucleotide repeat. Thus, in total 24% of the strains examined have the capacity to produce AutA. These observations indicate that the gene can be expressed but at a low frequency and suggest that *autA* expression is prone to phase variation at the AAGC repeats and to mutations.

Structure and variability of AutA

The *autA* gene from *N. meningitidis* MC58 is not expressed because of its number of AAGC repeats that renders the gene out of frame and the presence of a premature stop codon in the correct reading frame (Fig. S1B). Addition of one repeat unit and deletion of the premature stop codon results in an extended open reading frame (ORF) coding for a hypothetical protein of 695 aa with a signal peptide of 35 residues and a mature protein of 660 aa and a calculated molecular mass of 73 kDa (Fig. S1B). Classical monomeric ATs are usually much larger in size, up to ~ 3000 aa, and their passenger domains usually consist of a long β-helical backbone from which functional globular domains extend (Grijpstra *et al.*, 2013). An exception is the esterase EstA from *Pseudomonas aeruginosa* (Wilhelm *et al.*, 1999), which is of similar size as AutA (646 aa) and whose passenger is devoid of β-helical structure (van den Berg, 2010). Modelling of the three-dimensional structure of AutA indicated that its passenger domain (aa 35–385) can be divided into two regions (Fig. 1). The N-terminal part (aa 35–257) is predicted to consist of α-helices connected by loops of diverse length and shows only very limited homology to proteins of known structure. The C-terminal part (aa 257–385) is predicted to form a right-handed β-helix that probably constitutes the autochaperone domain, as evidenced by similarities with the crystal structures of the autochaperone domains of, for example, IcsA of *Shigella flexneri* (99.9% confidence) or IgA1 protease of

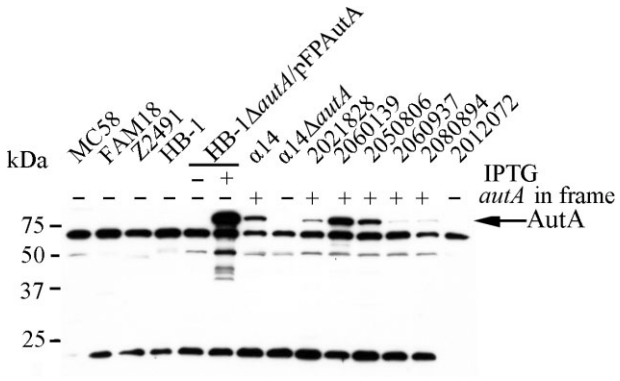

Fig. 2. Analysis of AutA expression. Western blot containing cell envelopes preparations of various *N. meningitidis* strains were probed with an antiserum directed against AutA. HB-1Δ*autA* carrying pFPAutA was grown in the presence or absence of 100 μM IPTG as indicated. Also indicated is whether the chromosomal *autA* gene is intact and in frame or not. Positions of molecular mass standards are shown at the left and that of AutA is marked at the right.

Haemophilus influenzae (99.7% confidence). Thus, like EstA, the passenger of AutA lacks an extended β-helical structure, but in contrast to EstA, it appears to contain the autochaperone domain. The translocator domain is predicted to form an α-helix (aa 386–415) inserted in a 12-stranded β-barrel (aa 415–695), showing significant similarity with the β-domains of various ATs (confidence 100%, data not shown).

To determine sequence conservation, DNA and protein sequences of AutA from 51 available *N. meningitidis* genomes were used (indicated in Table S1). Included were also one strain from *N. lactamica* and one from *N. polysaccharea*. Sequences with large numbers of stop codons or disruptions were not considered. Sequences alignments (see Fig. S2 for examples) showed that the sequence of the translocator domain was better preserved than that of the passenger, which, being surface exposed, is expected to be subjected to immune selection. Phylogenetic analysis of the predicted passenger domain in meningococcal strains indicated that strains from the same clonal origin were, in general, closely related (data not shown). In conclusion, AutA protein shows homologies with classical ATs, but the passenger domain, with exception of the autochaperone domain, seems to be unique.

Phase variation of autA in clinical isolates

We next investigated whether the expected phase variation at the AAGC repeats occurs in large sets of meningococcal disease isolates from the same genetic origin. If *autA* phase variation indeed occurs at high frequency, different isolates of the same cc should contain different numbers of repeats. We decided to focus on cc213 and cc32. In cc213 strain M01-240355, *autA* is not disrupted by a premature stop codon or other genetic elements (Table S1); thus, if this is a conserved feature of all cc213 strains, phase variation at the AAGC repeats will affect *autA* expression. In contrast, the *autA* genes of all cc32 strains analysed (Table S1) contain a well-conserved stop codon. Thus, in this case, variation in the number of repeats will not affect protein expression, but its evaluation will allow comparison of frequencies with cc213.

The repeat region of the *autA* gene was amplified by PCR with primers listed in Table S2 in a panel of 53 isolates of cc213 and 49 isolates of cc32 collected in the Netherlands between 2000 and 2010 from patients with meningococcal disease. The number of repeat units and the genetic characteristics of all isolates are listed in Table S3. The high variability of the surface-exposed loops of PorA and FetA in both sets of strains indicated that antigenic variation occurred at a high frequency. The number of repeat units in the *autA* genes ranged from 5 to 56, which is similar to the range (6–40) found in publicly available meningococcal genome sequences (Table S1). All isolates of cc213 lacked the premature stop codon downstream of the repeat region in the signal-sequence-encoding part of *autA*. In 15 out of 53 cc213 isolates (28%), *autA* was in phase, which matches the 33% expected if phase variation were a random process with no selection for in or out of phase during infection. Sequencing of the full-length gene in 10 of these isolates indicated the presence of a complete ORF with no amino-acid alterations relative to that of strain M01-240355. In 22 out of the 49 cc32 isolates (45%), *autA* was in phase, which is statistically not significantly different from the 28% observed in the cc213 strains. However, none of the cc32 isolates could express *autA* because all contained the premature stop codon in the same position as in *autA* of MC58.

Detection of AutA expression

To determine expression of AutA, Western blotting experiments were performed with a polyclonal antiserum raised against a fragment of the predicted passenger of AutA of strain HB-1, an unencapsulated derivative of H44/76. These experiments revealed a band of ~ 68 kDa in cell envelope preparations of all meningococcal strains examined (Fig. 2), including MC58, FAM18, Z2491 and HB-1, which were not expected to express AutA (Table S1). This band, which has a slightly lower apparent molecular weight than expected (73 kDa), was also detected in the *autA* deletion strain HB-1Δ*autA* and thus must represent a cross-reacting band. To identify the proper band, plasmid pFPAutA was introduced in strain HB-1Δ*autA*. The antiserum recognized a ~ 76 kDa

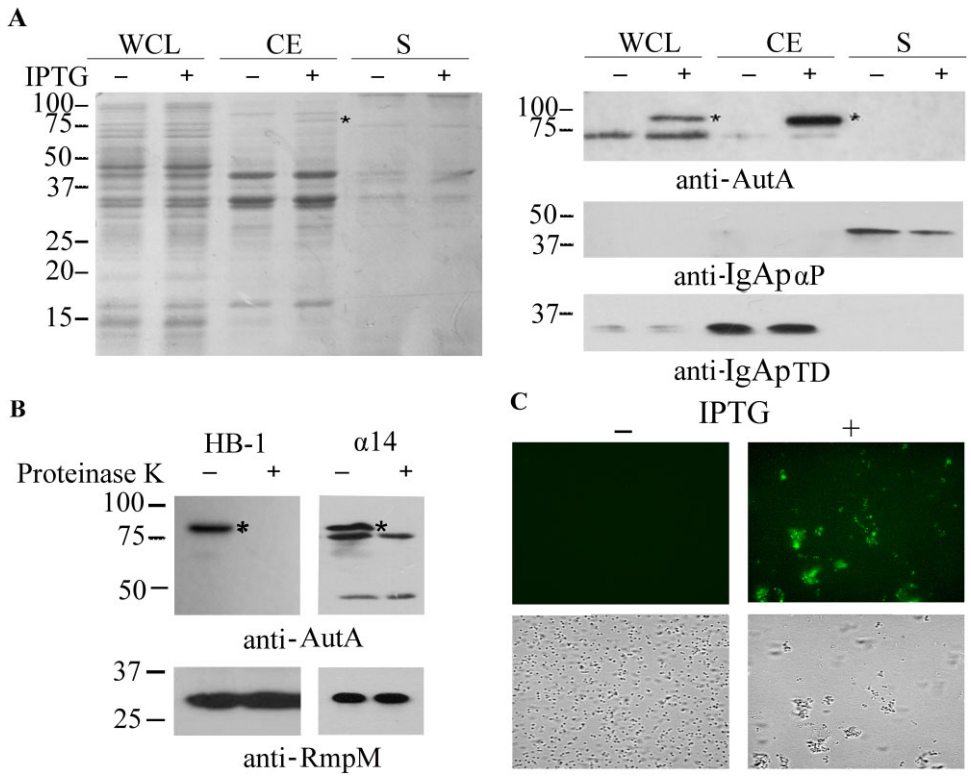

Fig. 3. Localization of AutA.
A. Proteins in whole cell lysates (WCL), cell envelopes (CE) and supernatants (S) of HB-1Δ*autA* carrying pFPAutA were separated by SDS-PAGE followed by Coomassie staining (left panel) or by Western blotting using antisera directed against AutA, the α-peptide of IgA protease (anti-IgAp αP) or the translocator domain of IgA protease (anti-IgAp TD) as indicated underneath the blots (right panel). The cells were grown in the presence or absence of IPTG as indicated. AutA is indicated with asterisks.
B. Protease accessibility assay. Intact cells of strain HB-1Δ*autA* carrying pFPAutA (HB-1) grown in the presence of IPTG and strain α14 were treated or not with proteinase K, and degradation of AutA, and RmpM was assessed by Western blotting. AutA is marked with an asterisk.
C. Immunofluorescence microscopy. HB-1Δ*autA* carrying pFPAutA was grown in the presence or absence of 100 μM IPTG and labelled with anti-AutA antiserum and FITC-labelled goat anti-rabbit IgG as the secondary antibody (top panels). Bright field images (lower panels) show the presence of cells.

band in cell envelope preparations of the resulting strain when it was cultured in the presence of IPTG (Fig. 2). A band of similar size was also detected in strain α14, which was expected to express *autA* from the chromosome, but not in an *autA* mutant derivative of this strain (Fig. 2). Bands of similar size were also detected in all disease isolates of cc213 examined in which the *autA* gene is in phase but not in those where the gene is out of phase (see Fig. 2 for examples). Interestingly, the intensity of the signal detected on the blots was different between these isolates. Sequence analysis revealed no differences in the coding regions (Fig. S2) or the promoter regions (data not shown) of the corresponding *autA* genes. Hence, we have no clear explanation for the different expression levels at the moment. Together, these analyses demonstrate, for the first time, that AutA is expressed in at least some *N. meningitidis* strains but not in reference strains like MC58 and Z2491.

The passenger of AutA is cell surface exposed

To determine whether the passenger domain of AutA is released into the extracellular medium, proteins present in whole cell lysates, cell envelopes and culture supernatants of strain HB-1Δ*autA* carrying pFPAutA were analysed by SDS-PAGE and Western blotting (Fig. 3A). The expected 76 kDa band was detected in the cell envelope preparations when *autA* expression was induced (Fig. 3A). No IPTG-dependent differences were detected in the protein profiles of the supernatant. As a control for the fractionation, we examined the same samples for the presence of the translocator domain and the α-peptide of the IgA protease. The α-peptide is a part of the passenger of IgA protease that is released into the medium when NalP is expressed (Roussel-Jazédé *et al.*, 2014). As expected, we detected the α-peptide in the spent medium and the translocator domain in the cell envelope fraction (Fig. 3A, right panel).

To test whether the passenger domain is localized at the cell surface, its proteinase K accessibility was assessed in intact bacteria. Proteinase K indeed cleaved AutA in intact cells of both strain HB-1Δ*autA* overexpressing AutA from pFPAutA and strain α14 expressing AutA from the chromosome, but it did not affect RmpM, a periplasmically exposed outer membrane protein, indicating that the integrity of the outer membrane was unaffected (Fig. 3B). Cell surface exposure of AutA was confirmed by immunofluorescence microscopy in HB-1Δ*autA* carrying pFPAutA (Fig. 3C). Thus, the passenger of AutA is secreted across the outer membrane but remains attached via the translocator domain to the cell surface.

AutA mediates bacterial aggregation

In the immunofluorescence microscopy experiments, we noticed that the AutA-expressing meningococci formed aggregates (Fig. 3C), suggesting a role for AutA in autoaggregation. To test whether AutA has such a role, we evaluated first the autoaggregation characteristics of wild-type strains. Bacteria from standing cultures showed a settling pattern that could be followed spectrophotometrically by measuring the optical density (OD) in the top of the tubes (Fig. S3). AutA$^+$ strain α14 was considerably more autoaggregative than AutA$^-$ strain HB-1. We then determined the effect of AutA expression on autoaggregation in isogenic strains. As expected, AutA expression from pFPAutA in HB-1Δ*autA* resulted in a fast settling of the bacteria, which was readily observed by visual inspection of the tubes and was not observed in the case of bacteria bearing a control plasmid (Fig. 4A). Similarly, AutA promoted autoaggregation in strain α14 as evidenced by a faster settling of the wild-type strain as compared with its *autA* mutant derivative, although the difference was smaller than observed in the case of the HB-1 derivatives (Fig. 4A). Light microscopy confirmed the presence of large aggregates in the cultures of both strains when AutA was expressed (Fig. 4B).

Next, we wanted to investigate the mechanism of aggregation. Proteins and DNA have been reported to play a role in interbacterial and bacteria–surface interactions. Thus, we treated cultures of bacteria expressing AutA with proteinase K or DNase I. Treatment with proteinase K fully inhibited AutA-mediated autoaggregation (Fig. 4C) in agreement with the sensitivity of AutA to the protease (Fig. 3B). Also treatment of AutA-expressing cells with DNase I inhibited autoaggregation but to a lesser extent (Fig. 4C). Similarly, DNase I treatment inhibited autoaggregation of α14 to levels of the *autA* mutant derivative (data not shown). Together, these data suggest that AutA mediates autoaggregation by interacting, directly or indirectly, with DNA.

To gain more insight into the role of eDNA in autoaggregation, we wished to determine whether AutA expression also promotes aggregation of bacteria in which the initiation of biofilm formation is independent of eDNA, such as cc11 strain BB-1 (Arenas *et al.*, 2013). Sequencing of the repeat region with the primers listed in Table S2 showed that BB-1, although its *autA* is in phase (26 repeat units), does not express AutA because of the presence of a premature stop codon. Repeated attempts to introduce pFPAutA into this strain failed for unknown reasons. Therefore, we integrated the *autA* gene together with the *lac* promoter and the *lacI*^{q} gene from pFPAutA into the *hrtA* region on the chromosome of BB-1. Western blotting confirmed the IPTG-inducible expression of AutA in the resulting strain (data not shown). Settling experiments demonstrated that AutA expression induced autoaggregation, which, however, was insensitive to DNase treatment in this strain (Fig. 4C, right panel). Thus, like in biofilm formation, the role of eDNA in AutA-mediated autoaggregation is strain dependent.

AutA impairs bacterial lattice formation

Previously, we showed that *N. meningitidis* forms visible lattice structures when grown for at least 12 h in six-well plates under static conditions (Arenas *et al.*, 2013). Strain HB-1 forms lattices constituted by large interconnected aggregates with intervening spaces, following a branch-like organization. This organization is dependent on DNA, as it can be disrupted by adding DNase I to the medium. Because AutA is involved in autoaggregation, we considered the possibility that its expression affects lattice formation. In the absence of IPTG, strain HB-1Δ*autA* carrying pFPAutA generated lattices after 24 and 48 h of incubation with a similar organization as observed previously for strain HB-1 (Fig. 5). IPTG-induced expression of AutA completely abolished this organization; the bacteria were organized in microcolonies that were mostly distributed at the border of the wells as was most evident after 48 h of incubation (Fig. 5). These data show that AutA expression modifies interbacterial interactions and induces a strong aggregation to form microcolonies.

We also analysed the influence of AutA on lattice formation in strain α14, which naturally expresses *autA* from the chromosome. No lattice structures were observed in the case of the wild-type bacteria, even not after 60 h of incubation, but the population was organized in a large number of microcolonies (Fig. 5). In contrast, the amount of microcolonies was reduced in the case of the *autA* mutant of α14, and defined lattice structures were observed after 60 h (Fig. 5). Thus, in spite of some differences in the manifestation of the lattice structures in both genetic backgrounds, these results demonstrate that

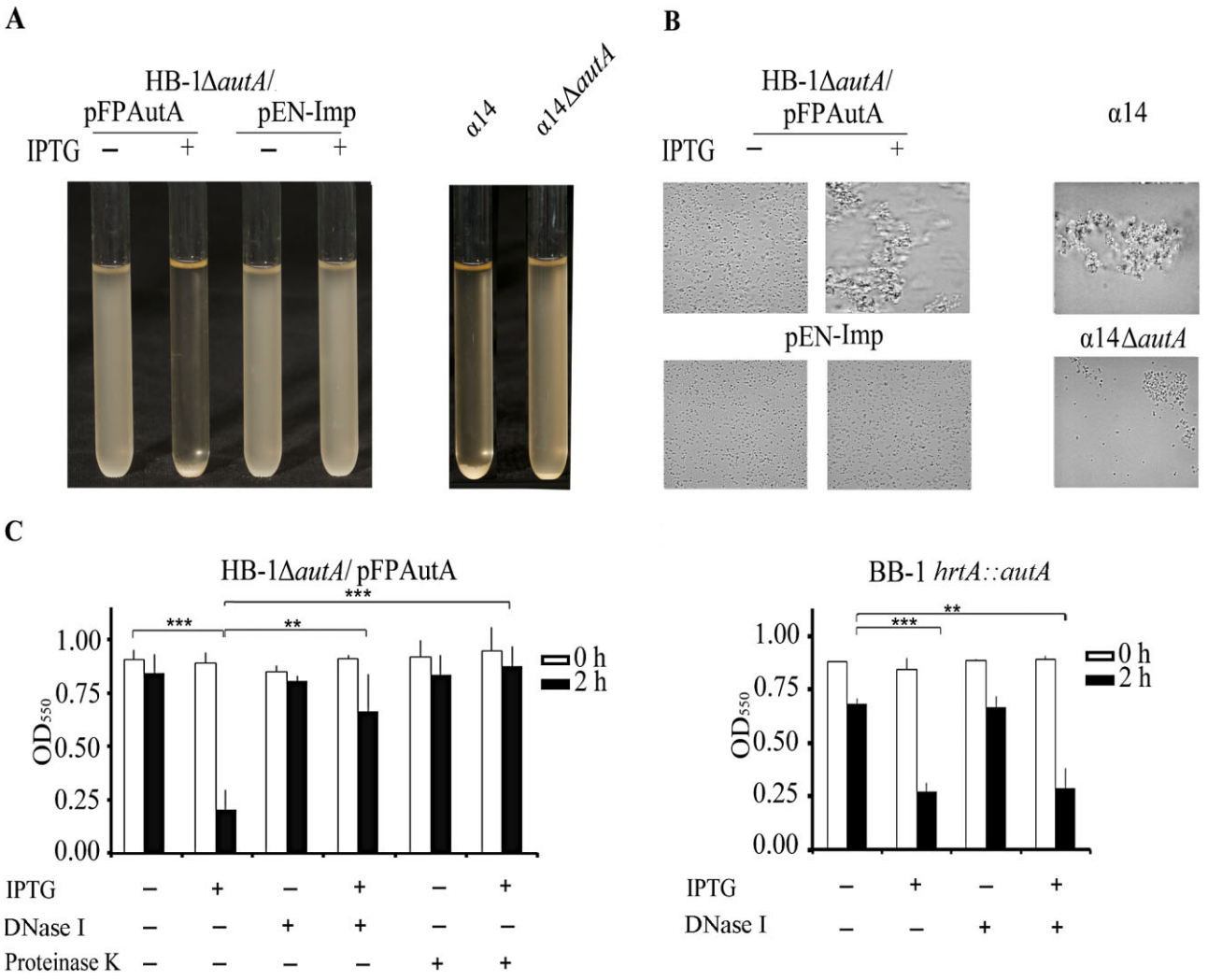

Fig. 4. AutA mediates autoaggregation.
A. Macroscopic views of settling assays. Overnight cultures of HB-1Δ*autA* carrying pFPAutA or, as a control, pEN-Imp, grown with or without IPTG, and of α14 and α14Δ*autA* were adjusted to the same OD_{550}, left standing for 2 h and then photographed.
B. The cultures that had been left standing for 2 h were vigorously mixed. Aliquots were spotted on microscopy slides and observed by phase-contrast microscopy. Representative pictures are shown (magnification × 1000).
C. Proteinase K and DNase I treatment inhibit settling. Cultures of HB-1Δ*autA* carrying pFPAutA (left panel) or BB-1 *hrtA::autA* (right panel), grown overnight in the presence of IPTG, were adjusted to an OD_{550} of 1 after which proteinase K or DNase I was added, and the cultures were left standing. The OD_{550} at the top of the cultures was measured at time 0 (white bars) and after 2 h (black bars). Data represent averages and standard variation of at least three independent experiments. Statistically significant differences were calculated by unpaired *t*-test and are marked at $^{**}P < 0.005$ and $^{***}P < 0.0005$.

AutA-mediated autoaggregation drastically impacts on lattice formation.

AutA alters biofilm formation

Because meningococcal lattice structures are related to biofilm architectures, we next investigated whether AutA expression also affects biofilm formation. Biofilm formation was first studied under static growth conditions in polystyrene plates and quantified by crystal-violet staining. In the absence of IPTG, strain HB-1Δ*autA* carrying pFPAutA formed biofilms similarly as did the wild-type strain (data not shown). Induction of AutA expression from the plasmid significantly reduced biofilm biomass, while this was not the case in bacteria bearing a control plasmid (Fig. 6A). Thus, AutA expression affects biofilm formation.

Next, we investigated the influence of AutA on biofilm organization under flow conditions, which allows for continuous monitoring of biofilm development by real-time fluorescence microscopy. After 14 h of growth, biofilms of strain HB-1 are constituted of large interconnected

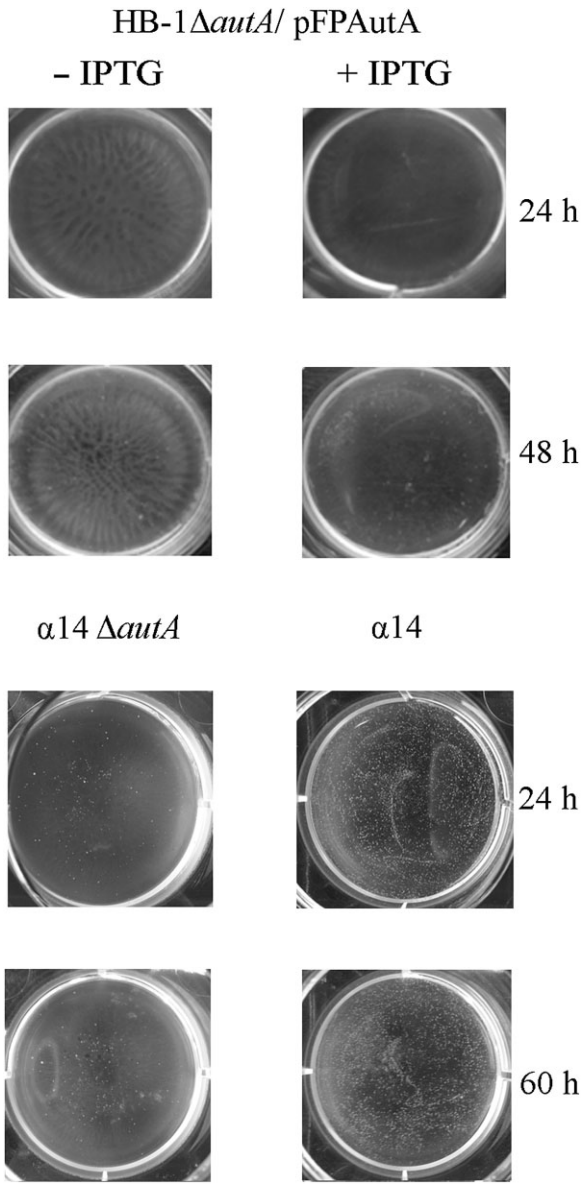

Fig. 5. Bacterial lattice formation. HB-1Δ*autA* carrying pFPAutA, α14 and α14Δ*autA* were pre-cultured in TSB while shaking. The HB-1Δ*autA* derivative was grown with and without IPTG as indicated. After 4 h of growth, the OD_{550} was adjusted to 0.1, and bacterial suspensions were transferred into six-well plates and incubated at 37°C under static conditions. The lattices formed were photographed after 24, 48 or 60 h as indicated with a conventional camera.

aggregates with intervening spaces between the biomass (Arenas *et al.*, 2013). In the absence of IPTG, biofilms of strain HB-1Δ*autA* carrying pFPAutA were formed very similarly as previously described for strain HB-1 (Video Clip S1), and the 14 h-old biofilms had a very similar architecture (Fig. 6B). Expression of AutA altered biofilm development considerably (Video Clip S2). Biofilms formed after 14 h were also constituted of large aggregates, which were, however, not interconnected (Fig. 6B). This organization reduced the coverage of the substratum, in agreement with the reduction of biofilm formation observed under static conditions (Fig. 6A). Statistical analysis of image stacks acquired by confocal microscopy of live/dead-stained biofilms using the COMSTAT software revealed a significantly higher roughness coefficient when AutA was expressed (Fig. 6C). Interestingly, also the surface to volume ratio was statistically higher in the $AutA^+$ strain (Fig. 6C). This parameter reflects what fraction of the biofilm is directly exposed to the nutrient flow (Heydorn *et al.*, 2000) and will be higher if many small structures are present compared with a few large structures. In contrast, biofilm biomass and thickness were not statistical different (Fig. 6C and data not shown), although the total biomass was lower when AutA was expressed, but probably the high variation of data, particularly for the $AutA^-$ cells, did not provide enough confidence for the test ($P = 0.13$).

Biofilms were also analysed of strain α14, which naturally expresses chromosomal *autA*, and its *autA* mutant derivative. Strain α14 formed biofilms constituted of bacterial aggregates of different sizes surrounded by free space, thus creating a non-interconnected structure (Fig. 6B). These images and comparison of structural biofilm parameters clearly evidence that HB-1 and α14 produce different biofilm structures. Deletion of *autA* from α14 generated biofilms constituted of smaller aggregates with reduced intervening spaces (Fig. 6B), creating a more interconnected structure compared with the wild type. Comparison of biofilm parameters using COMSTAT analysis revealed a statistically significant higher biomass and a reduced surface to volume ratio for the α14 *autA* mutant (Fig. 6C). Thickness and roughness coefficient were not statistically different between both strains, but the roughness coefficient was lower when AutA was not expressed (Fig. 6C); large data variation seems to be the reason of lack of statistical differences. Together, these assays showed that AutA expression significantly alters biofilm development and morphology in both genetic backgrounds and confirmed that AutA strongly enhances microcolony formation.

AutA is a self-associating AT that binds DNA

We hypothesized that AutA-mediated aggregation could involve one or a combination of different molecular interactions: (i) direct interaction between AutA molecules on the surfaces of neighbouring cells, (ii) interaction of AutA with another surface-exposed component on neighbouring cells and (iii) binding of cells via AutA to eDNA,

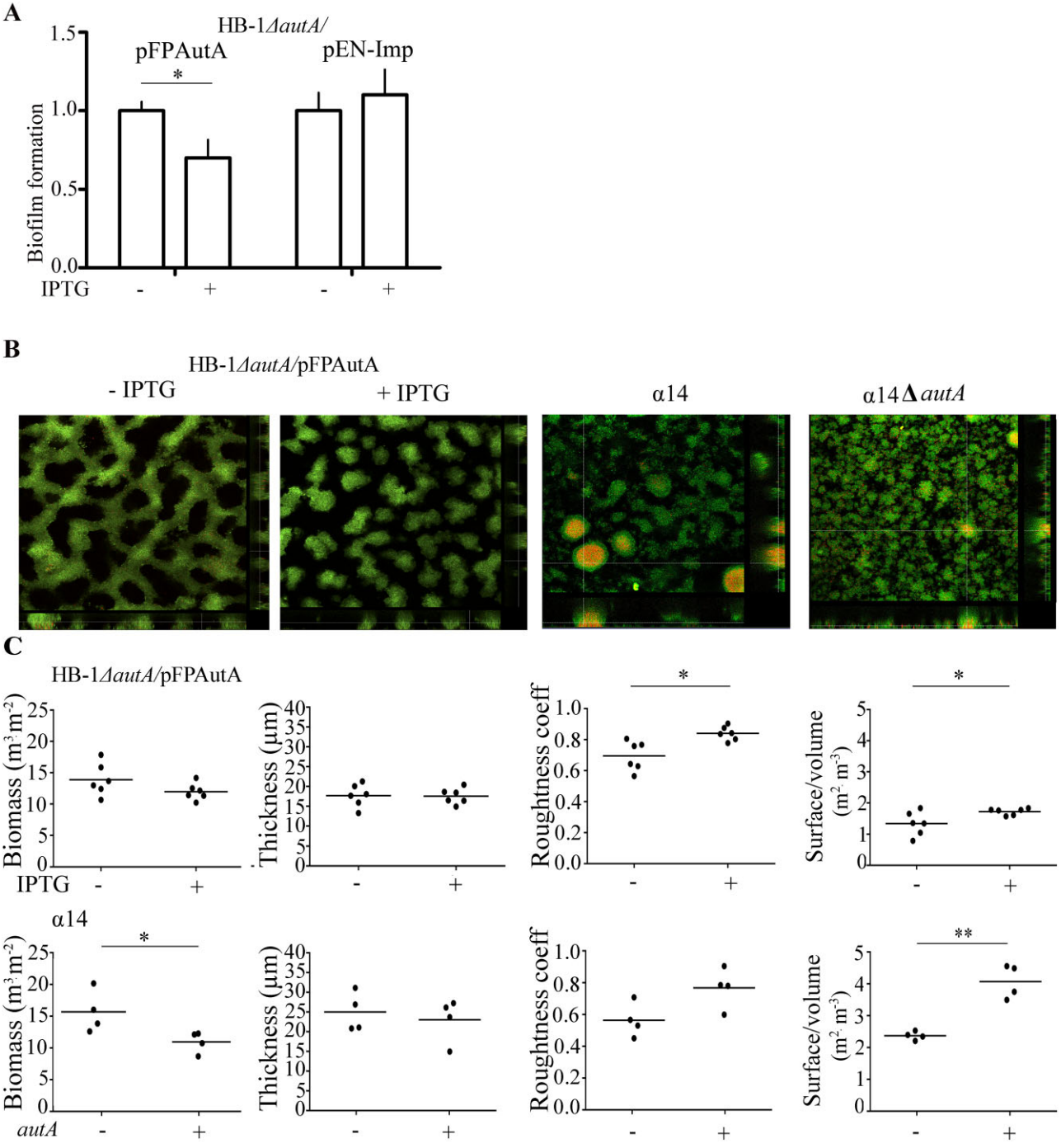

Fig. 6. Impact of AutA expression on biofilm formation.
A. Initial biofilm formation under static conditions. HB-1Δ*autA* carrying pFPAutA or, as a control, pEN-Imp was pre-cultured in TSB with or without IPTG. Aliquots of the cultures were transferred into 24-well plates and further incubated under static conditions. The biofilms formed were quantified after staining with crystal violet by measuring the OD_{630}. The data represent means and standard deviations of at least three independent experiments, and values are given as relative to the cultures without IPTG, which were set at 1.0. Statistically significant differences are marked with one asterisk (unpaired *t*-test of $P < 0.05$).
B. Biofilm formation under flow conditions. The architectures of 14 h-old biofilms formed by strain HB-1Δ*autA* carrying pFPAutA grown in the presence and absence of IPTG and by α14 and its *autB* mutant derivative are shown. Bacteria were stained with live/dead staining for optimal visualization.
C. Biomass, thickness, roughness coefficients and surface/volume ratios of biofilms were calculated using COMSTAT software. Values are means of data from at least six image stacks of one representative experiment of at least four independent replicates. Statistically significant differences between groups were calculated by unpaired *t*-test and are marked with one asterisk ($P < 0.05$) or two asterisks ($P < 0.005$).

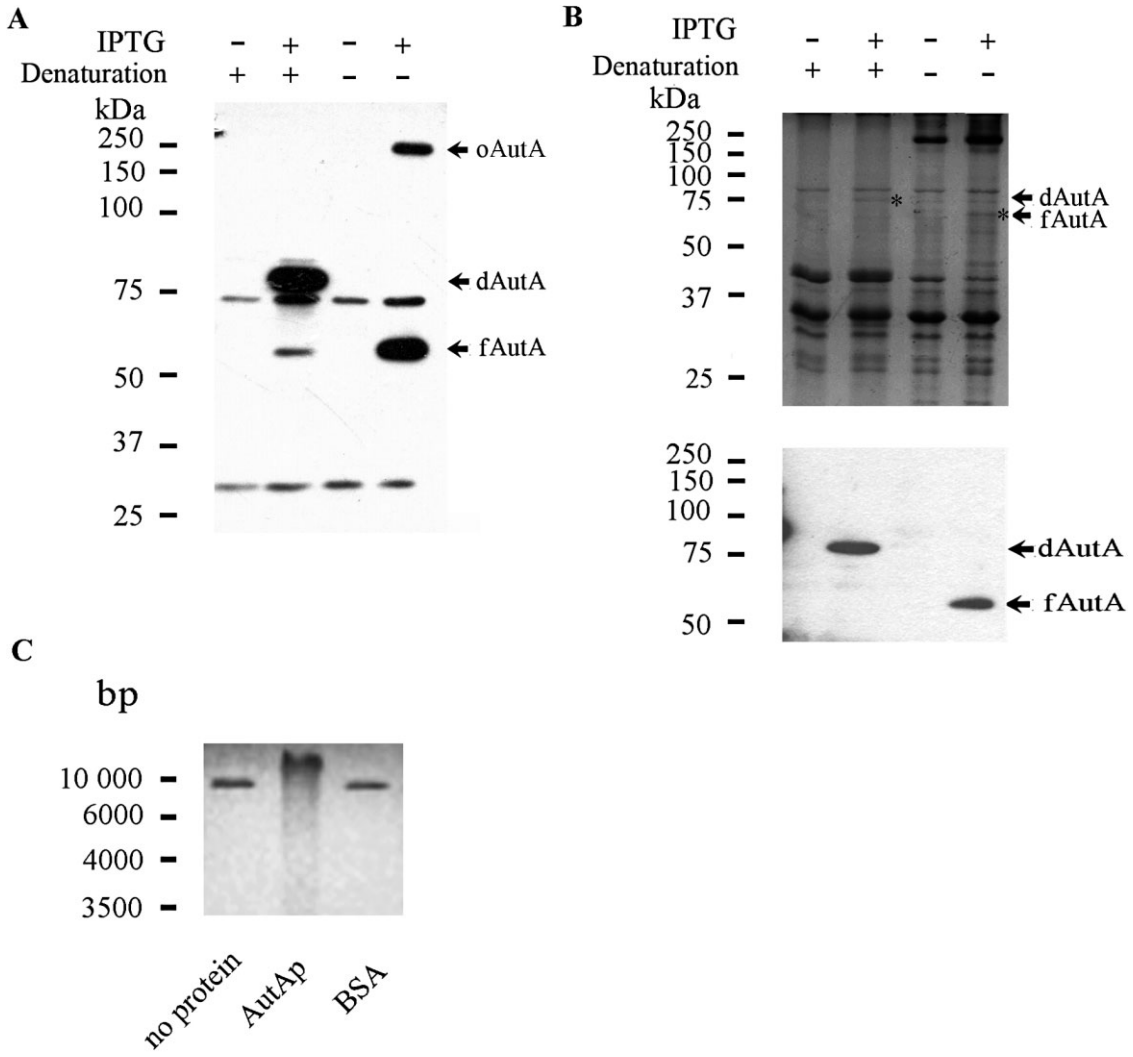

Fig. 7. Molecular interactions of AutA.
A. Western blot analysis of cell envelopes from strain HB-1Δ*autA* carrying pFPAutA grown in the presence or absence of IPTG using antiserum directed against AutA. Cell envelopes were analysed either under denaturating or non-denaturating conditions as indicated. The positions of denatured AutA (dAutA), folded AutA (fAutA) and of a possible oligomeric form of AutA (oAutA) are indicated.
B. Far-Western blot analysis. Cell envelopes of strain HB-1Δ*autA* carrying pFPAutA, grown in the presence or absence of IPTG, were separated by SDS-PAGE under denaturing or non-denaturing conditions. A Coomassie-stained gel is shown in the upper panel. The proteins were transferred from the gel to a nitrocellulose membrane, and after blocking, the membrane was incubated with 400 μg of His-tagged AutA passenger and then, after washing, with anti-His-tag antibody (lower panel). The positions of dAutA and fAutA are indicated with arrows and asterisks. Molecular mass standards are indicated at the left.
C. Electrophoretic mobility shift assay with 450 ng of the linearized plasmid pKO*nhbA-kan* (lane 1) incubated for 1 h at room temperature with 10 μg of His-tagged AutA passenger (lane 2) or BSA (lane 3).

although this latter possible mechanism does not appear to be involved in the case of strain BB-1. To investigate whether AutA can interact with itself or with other proteins in the outer membrane, we first analysed cell envelopes from HB-1Δ*autA* carrying pFPAutA by SDS-PAGE and Western blotting. Analysis of preparations under denaturing or non-denaturing conditions revealed a different electrophoretic mobility of AutA (Fig. 7A), in agreement with the heat-modifiable electrophoretic mobility of outer membrane proteins (Nakamura and Mizushima, 1976). Interestingly, an additional band with an apparent molecular weight of ~ 250 kDa was recognized by the antiserum in the non-denatured sample (Fig. 7A). This band suggested that AutA forms protein complexes. To identify the interacting partner of AutA, the complete passenger domain carrying an N-terminal His tag was expressed in and purified from *Escherichia coli*. Far-Western blotting assays were then used to identify interacting partners. To this end, cell envelope proteins were separated by SDS-PAGE and blotted to a nitrocellulose

membrane. The blot was then first incubated with the purified His-tagged AutA passenger, and binding of this protein to immobilized proteins on the blot was subsequently detected with anti-His antibodies. The purified AutA passenger was found to bind specifically to AutA on the blot both in denatured and non-denatured cell envelope preparations and not to any other protein present on the blots (Fig. 7B). This analysis shows that AutA is a self-associating AT.

Based on the observation that DNase I inhibited AutA-mediated autoaggregation in the HB-1 background (Fig. 4C), we tested whether AutA can also bind DNA. To this end, DNA electrophoretic mobility shift assays were performed using the purified His-tagged AutA passenger. Indeed, the recombinant protein retarded the migration of the target DNA on agarose gels (Fig. 7C). No gel shift was observed when the DNA was incubated with BSA as a control. This result demonstrates that AutA directly binds DNA.

Discussion

Hitherto, AutA had been poorly studied, and its expression was controversial. Ait-Tahar and colleagues (2000) observed that antibodies raised against full-length AutA recognized a ~ 68 kDa protein band in cell lysates of MC58, SD and Z2491. However, study of the *autA* gene in the available genome sequences of MC58 and Z2491 showed that the gene is out of phase by the number of tetranucleotide repeats in the signal-sequence-encoding part and that it contains a stop codon in the correct reading frame slightly further downstream (Peak *et al.*, 1999; van Ulsen and Tommassen, 2006). Ait-Tahar and colleagues assigned an alternative ATG start codon located downstream of the tetranucleotide repeat and the premature stop codon. However, in this scenario the AutA protein would be produced without a signal sequence, and it would therefore not be secreted. Because no *autA* mutant was included in the Western blots in that study (Ait-Tahar *et al.*, 2000), the identity of the observed 68 kDa band is questionable. In our work, we confirm that the *autA* gene is disrupted by various genetic features in many meningococcal and other neisserial strains. However, it can be expressed in at least some meningococcal strains, where its expression is prone to phase variation. In many of the currently available neisserial genome sequences, the *autA* gene is annotated with the previously proposed incorrect ATG start codon. We suggest that future genome annotations should consider the genetic elements described in this work.

Phase variation by slipped-strand mispairing at simple nucleotide repeats is often associated with the expression of surface molecules that are necessary for colonization or persistence of a pathogen in the host. This variation can be also related with tissue tropism, adaptation to environmental changes and immune evasion (Robertson and Meyer, 1992). Peak and colleagues (1999) first showed that *autA* contains an AAGC repeat motif and that different *N. meningitidis* strains contain a variable number of these units. However, the strains used were from different genetic origins, and the study did not consider other disruptions that might abolish gene expression. Therefore, estimations of the frequency of phase variation and the possible synthesis of AutA protein cannot be extracted from this early work. In the present study, we showed that *autA* expression is subject to phase variation in isolates of a similar genetic origin. However, our *in silico* analysis revealed that *autA* expression is affected by other genetic features, i.e. stop codons, and insertion and deletions that alter the frame or remove regions relevant for the protein structure. The frequency of these disruptions among clinical isolates is very high. Therefore, only in a limited number of strains of certain cc, AutA can phase variably be expressed.

Autoaggregation has been associated with pathogenesis in many bacterial pathogens. Within organized structures, bacteria are more resistant to host defences, such as phagocytosis, than planktonic cells are (Ochiai *et al.*, 1993). Our results show that AutA induces autoaggregation with implications for microcolony formation. However, the generation of this putative virulence phenotype contrasts with the expression of AutA in only a limited number of invasive meningococcal strains as well as with its presence in commensal *Neisseria* species (Table S1). In line with this observation, we found no positive selection for AutA expression in bacterial clones isolated from patients with meningococcal disease (Table S3). Together, these results indicate that AutA is not required for virulence, even not in strains of cc213 where it can be expressed. Thus, at this point, one may speculate about the role of AutA in the meningococcal biology. Although the meningococcus is well known as a pathogen, the bacteria normally reside in the nasopharynx without causing any symptoms. Many bacteria that occupy this ecological niche form biofilms during colonization. Importantly, biofilms formed in *in vitro* models are constituted of large numbers of bacteria. However, biofilms observed *in vivo* in mucosal epithelial cell biopsies are rather small and mostly structured in microcolonies in many bacterial pathogens that colonize the nasopharynx, including *N. meningitidis* (Sim *et al.*, 2000). Therefore, the microcolony structure may have an important role in bacterial colonization and persistence. Our studies demonstrate that AutA production strongly alters biofilm morphology to a much more compact microcolony structure. Thus, it is tentative to speculate that AutA may be relevant during the carrier

stage rather than during infection, which is in line with the presence of the gene in commensal *Neisseria* species. If this hypothesis is correct, the analysis of large collections of meningococcal carrier isolates may reveal a higher frequency of strains able to express AutA than the strains studied here, which are mostly patient isolates often of highly invasive lineages. Such strains may lose the capacity to produce AutA under selection pressure of the immune system. The development of *in vivo* models to study meningococcal infection and carrier stage will eventually be required to verify the role of AutA suggested in this study.

Generally, similar mechanisms are used for bacterial aggregation and biofilm formation. In several bacteria, ATs mediate bacterial aggregation and biofilm formation via self-association (Klemm *et al*., 2006). Structural analysis of one of these self-associating ATs, Ag43 of *E. coli*, revealed a long L-shaped β-helical structure that could enable association between two molecules by a Velcro-like mechanism (Heras *et al*., 2014). Our far-Western blotting assays clearly demonstrate that AutA has the capacity to self-associate. Thus, autoaggregation could be mediated by interaction between AutA molecules on the surface of neighbouring cells. However, the interaction between AutA molecules must be different than in the case of Ag43 because a long β-helical domain is not present in AutA. Analysis of the structure of AutA will be required to reveal the mechanism of self-association.

Interestingly, eDNA appeared to be required for efficient AutA-mediated autoaggregation in strain HB-1 but not in strain BB-1. This observation parallels the eDNA dependency of biofilm formation in these strains (Arenas *et al*., 2013). In *N. meningitidis*, two different strategies of biofilm development have been described, an eDNA-dependent and an eDNA-independent one (Lappann *et al*., 2010b). Our model strain HB-1 uses the former strategy where eDNA appears to constitute the glue element that is bound by positively charged surface-exposed proteins, i.e. NHBA and the α-peptide of IgA protease (Arenas *et al*., 2013), thus mediating cell-to-cell and cell-to-substratum interactions. Strain BB-1 is of cc11. Strains of cc11 bind less DNA to the cell surface and follow an eDNA-independent strategy of biofilm formation (Lappann *et al*., 2010b). How biofilm formation in these strains is initiated is unknown. The parallel between the eDNA dependency of autoaggregation and biofilm formation in strains HB-1 and BB-1 suggests a common step between the two processes. Possibly, both processes require initial interactions leading to loose associations of bacterial cells. Dependent on the genetic background, this initial interaction may require eDNA or not and the capacity of AutA to bind DNA may help in their formation. These associations might subsequently be reinforced by AutA-mediated protein–protein interactions leading stable aggregates. However, this step is not required for biofilm formation as the initial associations may also bind directly to the substratum. Further research will be required to verify this model.

In conclusion, we identified the *autA* gene, encoding a hitherto uncharacterized AT of *N. meningitidis*, in a large collection of available neisserial genome sequences. The gene appears to be disrupted by premature stop codons, insertions and/or deletions in many strains. However, we demonstrated that AutA can be expressed at least in certain meningococcal clonal lineages, where its expression is prone to phase variation. AutA remains at the bacterial cell surface where it mediates autoaggregation with implications on biofilm formation. Therefore, this work shows the first complete characterization of this AT and contributes to the understanding of the organization of neisserial cell communities.

Experimental procedures

Bioinformatic analysis

The *autA* genes were identified in the available genome sequences of strains from various *Neisseria* spp. in BLAST searches using the sequence encoding the passenger domain of AutA from MC58 (locus tag NMB0312) as the input query. Also, the flanking genes in the MC58 genome were used. Comparisons and analysis of DNA sequences were first performed with CLONE MANAGER software (Scientific & Educational Software). A terminator sequence was predicted with public software (http://rna.igmors.u-psud.fr/toolbox/arnold/). For DNA sequence comparisons, the *autA* sequences with large insertions or deletions were excluded. Alignment of DNA sequences was performed in MAFFT version 6 (http://align.bmr.kyushu-u.ac.jp/mafft/online/server/). Phylogenetic analyses were performed using the neighbour-joining method with the available MEGA software version 4.0 (http://www.megasoftware.net/). For protein structure predictions, the *autA* sequence from the MC58 genome was altered by adding one AAGC repeat unit and deleting the premature stop codon, resulting in an extended ORF. Available public software (http://www.predisi.de) was used to predict the presence and cleavage site of the N-terminal signal sequence in the deduced amino-acid sequence. The mature protein sequence was used for tertiary structure predictions using the public web-based programs PHYRE2 (http://www.sbg.bio.ic.ac.uk/phyre2/html/page.cgi?id=index) and SWISS-MODEL (http://www.swissmodel.expasy.org). The C-terminal part, encompassing the β-barrel and the autochaperone domain, was modelled with both programs, while, because of its limited homology with known crystal structures of other proteins, the remaining N-terminal part was uniquely modelled with SWISS-MODEL. To complete the final model, models obtained for the C-terminal part were superimposed and combined with that predicted for the N-terminal part using the free available program COOT 0.6.1 (http://www2.mrc-lmb.cam.ac.uk/Personal/pemsley/coot/).

Bacterial strains and growth conditions

Meningococcal reference strains MC58 (Tettelin *et al.*, 2000), FAM18 (Bentley *et al.*, 2007), Z2491 (Parkhill *et al.*, 2000), H44/76 (Piet *et al.*, 2011) and α14 (Schoen *et al.*, 2008) belong to our laboratory collection. The unencapsulated derivates HB-1 (Bos and Tommassen, 2005) and BB-1 (Arenas *et al.*, 2013) of H44/76 and B16B6, respectively, have been described. A panel of 102 meningococcal strains isolated from patients suffering from meningococcal meningitis in the Netherlands (Table S3) was classified in clonal groups at the Netherlands Reference Laboratory for Bacterial Meningitis, Amsterdam, based upon determination of Multilocus Sequence Typing and subsequent comparison with the profiles in the meningococcal MLST database (http://pubmlst.org/neisseria/) developed by Keith Jolley and sited at the University of Oxford (Jolley and Maiden, 2010). All meningococcal strains were grown at 37°C on GC medium base (Difco) supplemented with IsovitaleX (Becton Dickinson) at 37°C in a candle jar. For liquid cultures, bacteria were diluted in Tryptic Soy Broth (TSB) medium (Beckton Dickinson) to an OD_{550} of 0.1 and incubated in 25 cm^2 polystyrene cell culture flasks or 125 ml square media bottles with constant shaking at 110 r.p.m. *Escherichia coli* strains DH5α and BL21(DE3) (Invitrogen) were grown in Luria–Bertani (LB) medium or LB agar and at 37°C. When required, the media were supplemented with antibiotics: kanamycin (100 μg ml^{-1}), chloramphenicol (25 μg ml^{-1} for *E. coli* and 10 μg ml^{-1} for *N. meningitidis*), gentamicin (100 μg ml^{-1}) or ampicillin (100 μg ml^{-1}). To induce protein expression, 0.1 mM of IPTG was added at the beginning of the logarithmic phase.

PCR analysis and sequencing of the autA gene

Genomic DNA was extracted and purified by standard methods (Maloy, 1990) and used as template in PCR reactions. Segments of *autA* were amplified by PCR with primers listed in Table S2. For all amplifications, at least two independent PCR reactions were performed using High Fidelity Polymerase (Roche Diagnostics GmbH, Germany) or DreamTaq-DNA Polymerase (Fermentas, UK). For purification of PCR products from agarose gels, the Wizard® SV Gel and PCR Clean-Up System (Promega Corporation) were used. Sequencing reactions were performed at the Macrogen sequencing service (Amsterdam). When required, sequences were assembled using the SeqMan II software (DNAstart).

Cloning and transformation

All PCR fragments used for cloning were obtained using the High Fidelity Polymerase from genomic DNA of strain HB-1 with primers described in Table S2. PCR fragments were purified and, in some cases, digested with restriction enzymes for which sites were included in the primers, to be subsequently cloned in appropriate vectors. To delete the complete *autA* gene from the chromosome, DNA fragments immediately upstream and downstream of the *autA* coding region were obtained by PCR and sequentially cloned into pKO*nhbA-kan* (Arenas *et al.*, 2013). The resulting plasmid contains a kanamycin-resistance cassette between the two regions and was called pKO*autA-kan*. To overexpress the partial (aa 145–335) or complete (aa 35–424) passenger domain of AutA, the DNA fragments were amplified and first cloned into pCRII-TOPO (Invitrogen) and then subcloned into pET16b (Invitrogen) resulting in plasmids pET16b-autApp and pET16b-autAFp respectively. To overproduce the AutA protein in *N. meningitidis*, the gene without the signal-sequence-encoding part was amplified by PCR and cloned into pCRII-TOPO. For subsequent cloning, an NdeI restriction site (nucleotides 2032–2037 relative to the start codon) was removed by introducing a silent mutation with the QuickChange Site-Directed Mutagenesis Kit (Invitrogen) according to the manufacturer's instructions. Next, the fragment was digested from the pCRII-TOPO clone and inserted into plasmid pFP10-c-*lbpA* (Pettersson *et al.*, 2006). The resulting plasmid, pFPAutA, contains the DNA encoding the signal sequence of LbpA in frame with the *autA* gene. Plasmid pEN-Imp (Bos *et al.*, 2004) was used as negative control in functional assays.

To express *autA* ectopically from the chromosome, it was integrated together with the *lac* promoter and the *lacI*^{q} gene into the *htrA* locus, which was reported to allow for a high rate of recombination (Claus *et al.*, 1998). To this end, we used plasmid phrtA_*rfp*, which was generated by inserting the *rfp* gene, amplified by PCR from plasmid pTH1 (R. Nijland, unpublished), into plasmid pCRT_A_hrtA (Roussel-Jazédé *et al.*, 2013) via MluI and PpuMI. Subsequently, a gentamicin-resistance cassette amplified by PCR from pYRC (Arts *et al.*, 2007) was inserted via PpuMI resulting in phrtA_gm_rfp. The entire *autA* gene with the promoter, *lacI*^{q}, and the erythromycin-resistance cassette was amplified by PCR from pFPAutA and inserted into phrtA_gm_rfp via SmaI and AatII. The resulting plasmid, called phrtA_AutA, was used to integrate *autA* into the chromosome via homologous recombination.

The correct insertion of all cloned fragments was confirmed by PCR and sequencing. *Neisseria meningitidis* was transformed with intact or linearized plasmids as described (Volokhina *et al.*, 2011), and transformants were selected in GC plates with appropriate antibiotics. The generation of knockout mutants was verified by PCR and, when appropriate, by Western blotting.

Purification of recombinant proteins and antiserum production

AutA passenger polypeptides with an N-terminal His-tag were produced in *E. coli* BL21(DE3) after induction with IPTG and purified as inclusion bodies that were solubilized in 8 M urea, 50 mM glycine (pH 8.0) (van Ulsen *et al.*, 2003). The protein band corresponding to a recombinant protein of 190 amino-acid residues (partial passenger) was excised from SDS-PAGE gels and used for the production of rabbit antiserum at Eurogentec (Liège, Belgium). The inclusion bodies of the recombinant full-length passenger domain of AutA were dialysed against 10 mM Tris-HCl (pH 7.6) and purified by nickel affinity chromatography using Ni-NTA Agarose (QIAGEN GmbH, Hilden). Protein concentrations were determined with the BCA assay kit (Thermo Fisher Scientific, Rockford, IL, USA).

Sample preparation, SDS-PAGE and Western blotting

Whole cell lysates and supernatants were prepared and adjusted as previously described (van Ulsen *et al.*, 2003). Cell envelopes were isolated by ultrasonic disruption of cells followed by ultracentrifugation (Volokhina *et al.*, 2009). Protein concentrations in cell envelope preparations were determined with the BCA assay kit. SDS-PAGE was performed on 14% or 12% polyacrylamide gels in a discontinuous buffer system. Before loading, samples were diluted in double-strength sample buffer containing SDS (2%, final concentration) and β-mercaptoethanol and heated for 10 min at 100°C. For non-denaturing SDS-PAGE, the sample buffer contained low SDS concentration (0.2%, final concentration) and no β-mercaptoethanol, and the samples were not heated before electrophoresis. Electrophoresis was performed at 200 V during ~ 45 min at room temperature or, in the case of non-denaturing SDS-PAGE, at 12 mA during ~ 180 min on ice. After electrophoresis, proteins were stained in the gels with Coomassie brilliant blue G250 or transferred to nitrocellulose membranes, which were subsequently incubated with PBS containing 0.1% (v/v) Tween 20 (PBS-T) and 0.5% (w/v) non-fat dried milk (PBS-T-M). Membranes were incubated overnight with antisera at working dilution and then with horseradish peroxidase-conjugated goat anti-rabbit or anti-mouse immunoglobulins. The anti-RmpM monoclonal antibody MN2D6D was a gift from Peter van der Ley, and rabbit antisera directed against the α-peptide and the translocator domain of IgA protease is described (Roussel-Jazédé *et al.*, 2014).

Far-Western blotting was performed as previously described (Arenas *et al.*, 2010) but with some modifications. In short, proteins were transferred from gels to nitrocellulose membranes, blocked with PBS-T-M, and incubated overnight with 400 μg of recombinant His-tagged AutA passenger in PBS-T-M at 4°C. After extensive washing in PBS-T-M, the blot was incubated for 4 h with anti-His monoclonal antibodies (Thermo Fisher Scientific). After extensive washing in PBS-T-M, blots were developed with the Pierce ECL Western Blotting Substrate.

Proteinase K accessibility assays

A 4 h-old bacterial culture was adjusted to an OD_{550} of 1 in TSB, treated with 20 μg ml^{-1} of proteinase K (Fermentas) and incubated for 1 h at 37°C. Next, cells were harvested by centrifugation (4500 *g* for 5 min) in an Eppendorf Centrifuge 5424, and protein degradation was examined by SDS-PAGE and Western blotting.

Immunofluorescence microscopy

Bacterial cells were fixed with 1% (v/v) formaldehyde as previously described (Arenas *et al.*, 2008). Fixed bacteria were washed and incubated at a concentration of 10^7 cells ml^{-1} in PBS-T containing 1% (w/v) BSA (PBS-T-BSA) at room temperature. Aliquots were then incubated with anti-AutA antiserum at 1:5000 dilution, washed and incubated with Alexa Fluor 488-conjugated goat anti-rabbit IgG (Molecular Probes). Aliquots of 15 μl were spotted on a microscopy slide and analysed on a Diaphot300 confocal krypton/argon laser-scanning microscope (Nikon). Controls using unstained bacteria were included to adjust the instrument for non-specific cell-associated fluorescence.

Settling experiments and lattice formation

For settling experiments, overnight cultures were adjusted to an OD_{550} of 1 in 15 ml glass tubes in a final volume of 10 ml. Tubes were left standing at room temperature, and samples were taken from the top to measure the OD_{550} after various time periods. Tubes were also photographed to illustrate the different settling patterns. Alternatively, tubes were vortexed after incubation, and 15 μl of the suspensions were spotted on a microscopy slide and evaluated by light microscopy. In some experiments, proteinase K (100 μg ml^{-1}) or DNase I (10 μg ml^{-1}, Sigma-Aldrich) were added to the bacterial suspensions before settling. For lattice formation, bacteria were grown in six-well plates under static conditions (Arenas *et al.*, 2013) and photographed after 24, 48 and 60 h.

Biofilm formation under static conditions

Biofilms were formed under static conditions as described previously (Arenas *et al.*, 2013). Briefly, bacteria from 4 h shaking cultures in TSB were adjusted to an OD_{550} of 1, and 500 μl samples were transferred into 24-well polystyrene plates (Corning Incorporated). After 1 h of incubation at 37°C, the culture was removed and the adherent bacteria were washed with de-ionized water. Biofilms were stained with 0.25% crystal violet for 2 min and washed with de-ionized water. Biofilms were solubilized in 33% of acetic acid and quantified by measuring the OD_{630}.

Biofilm formation under flow conditions, imaging and film preparation

Biofilms were formed under flow conditions as described previously (Arenas *et al.*, 2013). Briefly, biofilms were cultivated in three-channel flow cells for inverted microscopes (cover glass mounted at the underside) with channel dimensions of $1 \times 4 \times 40$ mm (BioCentrum-DTU, Denmark). The substratum for biofilm growth was a 24×50 mm borosilicate cover glass, size 1.5 (VWR International BV, the Netherlands). Bacteria were first cultured in TSB without IPTG, adjusted to an OD_{595} of 0.08 and injected into the flow chamber. After 1 h at 37°C, medium with or without IPTG was pumped at a flow rate of 0.33 mm s^{-1} by using a peristaltic pump (Ismatec IPC 16). To better visualize the biofilm architecture, biofilms were stained with LIVE/DEAD BacLight bacterial viability stain (Life Technologies Europe BV, the Netherlands) dissolved in Dulbecco's Phosphate-Buffered Saline (Lonza, USA). Microscopic examination of biofilms, image acquisition and film preparation were performed as described previously (Arenas *et al.*, 2013). Structural parameters of the biofilm (biomass, average thickness, roughness coefficient and surface to volume ratio) were analysed using COMSTAT program (Heydorn *et al.*, 2000).

Electrophoretic mobility shift assay

DNA-binding properties of purified proteins were determined as previously described (Arenas *et al.*, 2013). The target

DNA, plasmid pKO*nhbA-kan*, was first linearized with NcoI and then incubated with 40 μg of the full-length passenger of AutA or BSA as negative control. After electrophoresis on a 1% agarose gel, the DNA was stained with ethidium bromide.

Statistical analysis

For biofilm formation under static conditions and settling experiments, data from at least three independent experiments performed in duplicate were used for statistical analysis. For biofilm formation under flow conditions, six image stacks randomly generated of each sample were obtained from a representative experiment. Statistical comparisons were made using an unpaired statistical *t*-test with GRAPH PAD SOFTWARE (Graph Pad Software, Inc).

Nucleic acid accession numbers

The sequences of the *autA* genes of disease isolates of cc213 determined in this study (isolates 2081595, 2080894, 2080861, 2080309, 2050806, 2021828, 2040789, 2060937 and 2021590) were deposited in GenBank ID (KF952520, KF952521, KF952522, KF952523, KF952524, KF952525, KF952526, KF952527, KF952528).

Acknowledgements

We would like to thank Miguel Arenas (Consejo Superior de Investigaciones Científicas, Madrid) for assistance in bioinformatic analysis, Peter van Ulsen (Vrije Universiteit Amsterdam) for discussion and Jan Grijpstra for technical assistance and discussion. This work was supported by the Netherlands Organization for Health Research and Development (ZonMw) grant number 91206083.

References

Ait-Tahar, K., Wooldridge, K.G., Turner, D.P.J., Atta, M., Todd, I., and Ala'Aldeen, D.A.A. (2000) Auto-transporter A protein of *Neisseria meningitidis*: a potent $CD4^+$ T-cell and B-cell stimulating antigen detected by expression cloning. *Mol Microbiol* **37:** 1094–1105.

Arenas, J., Abel, A., Sánchez, S., Marzoa, J., Berrón, S., van der Ley, P., *et al*. (2008) A cross-reactive neisserial antigen encoded by the NMB0035 locus shows high sequence conservation but variable surface accessibility. *J Med Microbiol* **57:** 80–87.

Arenas, J., van Dijken, H., Kuipers, B., Hamstra, H.J., Tommassen, J., and van der Ley, P. (2010) Coincorporation of LpxL1 and PagL mutant lipopolysaccharides into liposomes with *Neisseria meningitidis* opacity protein: influence on endotoxic and adjuvant activity. *Clin Vaccine Immunol* **17:** 487–495.

Arenas, J., Nijland, R., Rodriguez, F.J., Bosma, T.N.P., and Tommassen, J. (2013) Involvement of three meningococcal surface-exposed proteins, the heparin-binding protein NhbA, the α-peptide of IgA protease and the autotransporter protease NalP, in initiation of biofilm formation. *Mol Microbiol* **87:** 254–268.

Arts, J., van Boxtel, R., Filloux, A., Tommassen, J., and Koster, M. (2007) Export of the pseudopilin XcpT of the *Pseudomonas aeruginosa* type II secretion system via the signal recognition particle-Sec pathway. *J Bacteriol* **189:** 2069–2076.

Bentley, S.D., Vernikos, G.S., Snyder, L.A.S., Churcher, C., Arrowsmith, C., Chillingworth, T., *et al*. (2007) Meningococcal genetic variation mechanisms viewed through comparative analysis of serogroup C strain FAM18. *PLoS Genet* **3:** e23.

van den Berg, B. (2010) Crystal structure of a full-length autotransporter. *J Mol Biol* **396:** 627–633.

Bos, M.P., and Tommassen, J. (2005) Viability of a capsule- and lipopolysaccharide-deficient mutant of *Neisseria meningitidis*. *Infect Immun* **73:** 6194–6197.

Bos, M.P., Tefsen, B., Geurtsen, J., and Tommassen, J. (2004) Identification of an outer membrane protein required for the transport of lipopolysaccharide to the bacterial cell surface. *Proc Natl Acad Sci USA* **101:** 9417–9422.

Capecchi, B., Adu-Bobie, J., Di Marcello, F., Ciucchi, L., Masignani, V., Taddei, A., *et al*. (2005) *Neisseria meningitidis* NadA is a new invasin which promotes bacterial adhesion to and penetration into human epithelial cells. *Mol Microbiol* **55:** 687–698.

Claus, H., Frosch, M., and Vogel, U. (1998) Identification of a hotspot for transformation of *Neisseria meningitidis* by shuttle mutagenesis using signature-tagged transposons. *Mol Gen Genet* **259:** 363–371.

Costerton, J.W., Lewandowski, Z., Caldwell, D.E., Korber, D.R., and Lappin-Scott, H.M. (1995) Microbial biofilms. *Annu Rev Microbiol* **49:** 711–745.

Criss, A.K., Kline, K.A., and Seifert, H.S. (2005) The frequency and rate of pilin antigenic variation in *Neisseria gonorrhoeae*. *Mol Microbiol* **58:** 510–519.

Grijpstra, J., Arenas, J., Rutten, L., and Tommassen, J. (2013) Autotransporter secretion: varying on a theme. *Res Microbiol* **164:** 562–582.

Heras, B., Totsika, M., Peters, K.M., Paxman, J.J., Gee, C.L., Jarrott, R.J., *et al*. (2014) The antigen 43 structure reveals a molecular Velcro-like mechanism of autotransporter-mediated bacterial clumping. *Proc Natl Acad Sci USA* **111:** 457–462.

Heydorn, A., Nielsen, A.T., Hentzer, M., Sternberg, C., Givskov, M., Ersbøll, B.K., and Molin, S. (2000) Quantification of biofilm structures by the novel computer program COMSTAT. *Microbiology* **146:** 2395–2407.

Jolley, K.A., and Maiden, M.C. (2010) BIGSdb: scalable analysis of bacterial genome variation at the population level. *BMC Bioinformatics* **11:** 595–606.

Klemm, P., Vejborg, R.M., and Sherlock, O. (2006) Self-associating autotransporters, SAATs: functional and structural similarities. *Int J Med Microbiol* **296:** 187–195.

Lappann, M., and Vogel, U. (2010) Biofilm formation by the human pathogen *Neisseria meningitidis*. *Med Microbiol Immunol* **199:** 173–183.

Lappann, M., Claus, H., van Alen, T., Harmsen, M., Elias, J., Molin, S., and Vogel, U. (2010) A dual role of extracellular DNA during biofilm formation of *Neisseria meningitidis*. *Mol Microbiol* **75:** 1355–1371.

Lin, L., Ayala, P., Larson, J., Mulks, M., Fukuda, M., Carlsson, S.R., *et al*. (1997) The *Neisseria* type 2 IgA1 protease

cleaves LAMP1 and promotes survival of bacteria within epithelial cells. *Mol Microbiol* **24:** 1083–1094.

Maloy, S.R. (1990) Jones and Bartlett series in biology. In *Experimental Techniques in Bacterial Genetics*. Stanion, L. (ed.). Boston, MA, USA: Jones and Bartlett Publishers, p. 180.

Nakamura, K., and Mizushima, S. (1976) Effects of heating in dodecyl sulfate solution on the conformation and electrophoretic mobility of isolated major outer membrane proteins from *Escherichia coli* K-12. *J Biochem* **80:** 1411–1422.

Ochiai, K., Kurita-Ochiai, T., Kamino, Y., and Ikeda, T. (1993) Effect of co-aggregation on the pathogenicity of oral bacteria. *J Med Microbiol* **39:** 183–190.

Oliver, D.C., Huang, G., Nodel, E., Pleasance, S., and Fernandez, R.C. (2003) A conserved region within the *Bordetella pertussis* autotransporter BrkA is necessary for folding of its passenger domain. *Mol Microbiol* **47:** 1367–1383.

Parkhill, J., Achtman, M., James, K.D., Bentley, S.D., Churcher, C., Klee, S.R., *et al*. (2000) Complete DNA sequence of a serogroup A strain of *Neisseria meningitidis* Z2491. *Nature* **404:** 502–506.

Peak, I.R., Jennings, M.P., Hood, D.W., and Moxon, E.R. (1999) Tetranucleotide repeats identify novel virulence determinant homologues in *Neisseria meningitidis*. *Microb Pathog* **26:** 13–23.

Peterson, J.H., Tian, P., Ieva, R., Dautin, N., and Bernstein, H.D. (2010) Secretion of a bacterial virulence factor is driven by the folding of a C-terminal segment. *Proc Natl Acad Sci USA* **107:** 17739–17744.

Pettersson, A., Kortekaas, J., Weynants, V.E., Voet, P., Poolman, J.T., Bos, M.P., and Tommassen, J. (2006) Vaccine potential of the *Neisseria meningitidis* lactoferrin-binding proteins LbpA and LbpB. *Vaccine* **24:** 3545–3557.

Piet, J.R., Huis in 't Veld, R.A.G., van Schaik, B.D.C., van Kampen, A.H.C., Baas, F., van de Beek, D., *et al*. (2011) Genome sequence of *Neisseria meningitidis* serogroup B strain H44/76. *J Bacteriol* **193:** 2371–2372.

Robertson, B.D., and Meyer, T.F. (1992) Genetic variation in pathogenic bacteria. *Trends Genet* **8:** 422–427.

Roussel-Jazédé, V., Grijpstra, J., van Dam, V., Tommassen, J., and van Ulsen, P. (2013) Lipidation of the autotransporter NalP of *Neisseria meningitidis* is required for its function in the release of cell-surface-exposed proteins. *Microbiology* **159:** 286–295.

Roussel-Jazédé, V., Arenas, J., Langereis, J., Tommassen, J., and van Ulsen, P. (2014) Variable processing of the IgA protease autotransporter at the cell surface of *Neisseria meningitidis*. *Microbiology* (in press).

Saunders, N.J., Jeffries, A.C., Peden, J.F., Hood, D.W., Tettelin, H., Rappuoli, R., and Moxon, E.R. (2000) Repeat-associated phase variable genes in the complete genome sequence of *Neisseria meningitidis* strain MC58. *Mol Microbiol* **37:** 207–215.

Scarselli, M., Serruto, D., Montanari, P., Capecchi, B., Adu-Bobie, J., Veggi, D., *et al*. (2006) *Neisseria meningitidis* NhhA is a multifunctional trimeric autotransporter adhesin. *Mol Microbiol* **61:** 631–644.

Schoen, C., Blom, J., Claus, H., Schramm-Glück, A., Brandt, P., Müller, T., *et al*. (2008) Whole-genome comparison of disease and carriage strains provides insights into virulence evolution in *Neisseria meningitidis*. *Proc Natl Acad Sci USA* **105:** 3473–3478.

Serruto, D., Adu-Bobie, J., Scarselli, M., Veggi, D., Pizza, M., Rappuoli, R., and Aricò, B. (2003) *Neisseria meningitidis* App, a new adhesin with autocatalytic serine protease activity. *Mol Microbiol* **48:** 323–334.

Serruto, D., Spadafina, T., Ciucchi, L., Lewis, L.A., Ram, S., Tontini, M., *et al*. (2010) *Neisseria meningitidis* GNA2132, a heparin-binding protein that induces protective immunity in humans. *Proc Natl Acad Sci USA* **23:** 3770–3775.

Sim, R.J., Harrison, M.M., Moxon, E.R., and Tang, C.M. (2000) Underestimation of meningococci in tonsillar tissue by nasopharyngeal swabbing. *Lancet* **356:** 1653–1654.

Tauseef, I., Ali, Y.M., and Bayliss, C.D. (2013) Phase variation of PorA, a major outer membrane protein, mediates escape of bactericidal antibodies by *Neisseria meningitidis*. *Infect Immun* **81:** 1374–1380.

Tettelin, H., Saunders, N.J., Heidelberg, J., Jeffries, A.C., Nelson, K.E., Eisen, J.A., *et al*. (2000) Complete genome sequence of *Neisseria meningitidis* serogroup B strain MC58. *Science* **287:** 1809–1815.

Turner, D.P.J., Wooldridge, K.G., and Ala'Aldeen, D.A.A. (2002) Autotransported serine protease A of *Neisseria meningitidis*: an immunogenic, surface-exposed outer membrane, and secreted protein. *Infect Immun* **70:** 4447–4461.

van Ulsen, P., and Tommassen, J. (2006) Protein secretion and secreted proteins in pathogenic *Neisseriaceae*. *FEMS Microbiol Rev* **30:** 292–319.

van Ulsen, P., van Alphen, L., ten Hove, J., Fransen, F., van der Ley, P., and Tommassen, J. (2003) A *Neisserial* autotransporter NalP modulating the processing of other autotransporters. *Mol Microbiol* **50:** 1017–1030.

van Ulsen, P., Adler, B., Fassler, P., Gilbert, M., van Schilfgaarde, M., van der Ley, P., *et al*. (2006) A novel phase-variable autotransporter serine protease, AusI, of *Neisseria meningitidis*. *Microbes Infect* **8:** 2088–2097.

Vidarsson, G., Overbeeke, N., Stemerding, A.M., van den Dobbelsteen, G., van Ulsen, P., van der Ley, P., *et al*. (2005) Working mechanism of immunoglobulin A1 (IgA1) protease: cleavage of IgA1 antibody to *Neisseria meningitidis* PorA requires de novo synthesis of IgA1 protease. *Infect Immun* **73:** 6721–6726.

Virji, M. (2009) Pathogenic *Neisseriae*: surface modulation, pathogenesis and infection control. *Nat Rev Microbiol* **7:** 274–286.

Volokhina, E.B., Beckers, F., Tommassen, J., and Bos, M.P. (2009) The β-barrel outer membrane protein assembly complex of *Neisseria meningitidis*. *J Bacteriol* **191:** 7074–7085.

Volokhina, E.B., Grijpstra, J., Stork, M., Schilders, I., Tommassen, J., and Bos, M.P. (2011) Role of the periplasmic chaperones Skp, SurA, and DegQ in outer membrane protein biogenesis in *Neisseria meningitidis*. *J Bacteriol* **193:** 1612–1621.

Wilhelm, S., Tommassen, J., and Jaeger, K.E. (1999) A novel lipolytic enzyme located in the outer membrane of *Pseudomonas aeruginosa*. *J Bacteriol* **181:** 6977–6986.

Yi, K., Rasmussen, A.W., Gudlavalleti, S.K., Stephens, D.S., and Stojiljkovic, I. (2004) Biofilm formation by *Neisseria meningitidis*. *Infect Immun* **72:** 6132–6138.

Supporting information

Additional Supporting Information may be found in the online version of this article at the publisher's web-site:

Fig. S1. Genetic context and organization of the *autA* gene in various *Neisseria* strains.
A. Comparison of the *autA* loci in the genome sequences of *N. meningitidis* strains MC58 and α153, *N. lactamica* strain 020-06, *N. gonorrhoeae* strain NCCP11945 and *N. flavescens* strain NRL30031/H210. Numbers at the side of each map indicate the first and last nucleotide position of the DNA fragment shown in accordance with genome annotations, and locus tags are provided. The (pseudo)genes (arrows) and intergenic regions (lines) with high sequence similarity are coloured identically in the different genomes. The gene upstream of *autA* (coloured red) is conserved in most *neisserial* genomes; it may encode a hypothetical protein of 81 aa, but in some strains an upstream-located start codon is assigned resulting in a larger protein. The gene downstream of *autA* (coloured green) is also well conserved and encodes a predicted outer membrane protein (annotated as OmpU in some genomes) involved in the colonization of the nasopharyngeal mucosa (Exley *et al*., 2009). In NRL30031/H210, the *autA* gene is flanked upstream by the *mdaB* gene (NEIFLAOT_02052) encoding a modulator of drug activity B; its homologue in MC58 is NMB1857. The gene downstream of *autA* (pale blue) encodes a hypothetical cytosolic protein, uniquely found in *N. flavescens* and *N. subflava*. Interestingly, the genes further upstream and downstream of the locus (NEIFLAOT _02053 and NEIFLAOT_02046, respectively) are homologous to the genes NMB2133 and the 3′ end of NMB2134 respectively. These genes are contiguous in the genome of MC58, suggesting that a DNA segment containing *autA* gene and the flanking genes was inserted in block in this region in *N. flavescens*. In this process, the 5′ end of the gene corresponding to NMB2134 was apparently lost. It is noteworthy that NMB2134 is homologous to *tamA* of *E. coli*, which was reported to be involved in AT secretion (Selkrig *et al*., 2012). Sequences 127 bp upstream and 366 bp downstream of *autA* are preserved in all the different genomic contexts, suggesting that these regions are co-transferred. Examination of these regions revealed sequences for a putative promoter and transcription terminator (see panel B), indicating that the gene is monocistronic. The 127 bp upstream region contains sequences of 47 and 26 bp in length that are variably repeated in direct and inverted orientation further upstream in all species except in *N. flavescens*. A blast search revealed the presence of multiple copies of these repeats all along the meningococcal chromosomes. These sequences share over 90% identity with known RS3 palindromic sequences. They are present, for example, upstream and downstream of the *porA* gene, where they are implicated in the loss of this gene in certain isolates via recombination (van der Ende *et al*., 1999). The coding region of the *autA* gene is segmented in three regions encoding the signal sequence (coloured solid black), the passenger domain (open striped) and the β-barrel domain at the 3′ end. In all genomes shown, the *autA* gene is out of frame because of the number of AAGC repeats in the signal-sequence-encoding region, and some of the genes are further disrupted by a well-conserved premature stop codon located in the same part (indicated by red slashes). Some of the genes contain various (additional) stop codons in the proper reading frame along the gene, i.e. in α153, NCCP11945 and NRL30031/H210 (not indicated for clarity reasons). In *N. meningitidis* α153, the *autA* gene contains an insertion of a transposable element of 843 bp (coloured blue) in the passenger domain. An insertion of the same element is also present in the *autA* genes of strains NM255 and NM2657 but at a different position as in α153, reflecting that they arose from an independent insertion events. In *N. gonorrhoeae*, the *autA* gene suffers a deletion of 983 nucleotides (indicated by discontinuous lines).
B. Relevant genetic elements in the *autA* gene in MC58. The relative positions of the predicted -35 box (TTGCGA), Pribnow box (TATAAT), ribosome-binding site (RBS) (AGGA), start codon, AAGC repeat region (black bar), premature stop codon (red slash), stop codon and the transcription terminator sequences (ACCGGCAGTTTCCCGCCGGT) are indicated at the bottom relative to the start codon (above the line) and according with coordinates of the MC58 genome sequence (beneath the line). The positions of the start codon annotated by Ait-Tahar and colleagues (2000) (ATG*), cleavage site for signal peptidase, and start and end of the passenger domain are also provided. The fragment of the passenger-encoding domain that was expressed for raising antiserum is indicated by a grey line.
Fig. S2. Alignment of the predicted mature AutA in various *N. meningitidis* strains. Numbers above the alignment indicate amino-acid positions according with the full-length sequence of MC58 AutA obtained when the gene is in frame and the premature stop codon is deleted. Asterisks, colons and periods below the sequences indicate identical amino acids in all aligned sequences, and positions with conserved and semi-conserved substitutions respectively. The start and end of the AutA segment that was used to raise antiserum are indicated.
Fig. S3. Analysis of autoaggregation in *N. meningitidis*. Suspensions from overnight cultures of strains HB-1, BB-1 and α14were adjusted to the same OD_{550} and left standing. The OD_{550} at the top of the tube was determined each 2 h.
Table S1. Identification and characterization of the *autA* gene in available *Neisseria* genome sequences. Homologues were identified in a BLASTnt search using as query the sequence encoding the AutA passenger domain of MC58. The gene locus, position on chromosome, number of tetranucleotide repeats in the 5′ region and the resulting in/out phase are given.
Table S2. Primers used in this study. Restriction sites used for cloning are indicated and underlined.
Table S3. Determination of the number of AAGC-repeat units in the *autA* gene of invasive isolates of *Neisseria meningitidis*.
Video Clip Biofilm formation of strain HB-1Δ*autA* carrying pFPAutA cultured in TSB medium without (Video Clip S1) or with IPTG (Video Clip S2) developed under flow systems.